Propagation and Dissipation of MHD Waves in Coronal Holes

B.N. Dwivedi

Banaras Hindu University, Varanasi-221005, India.

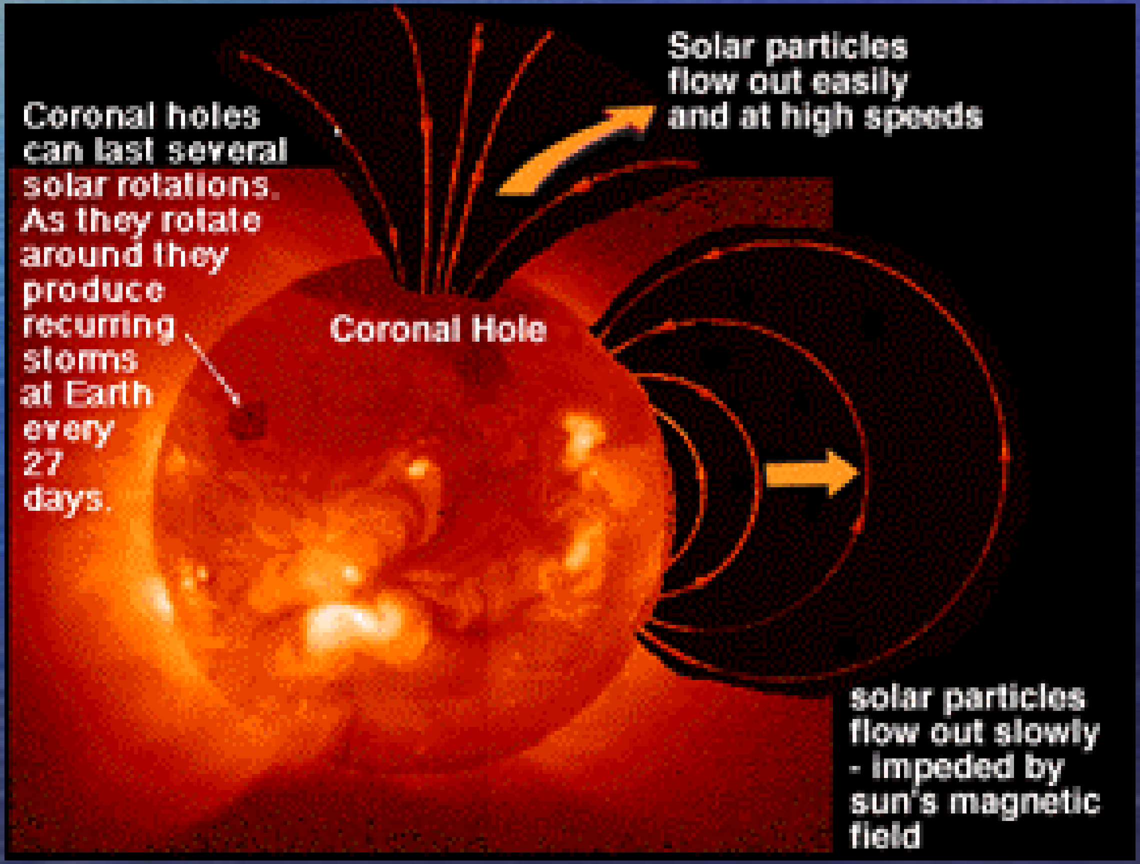

Solar Wind Source Region

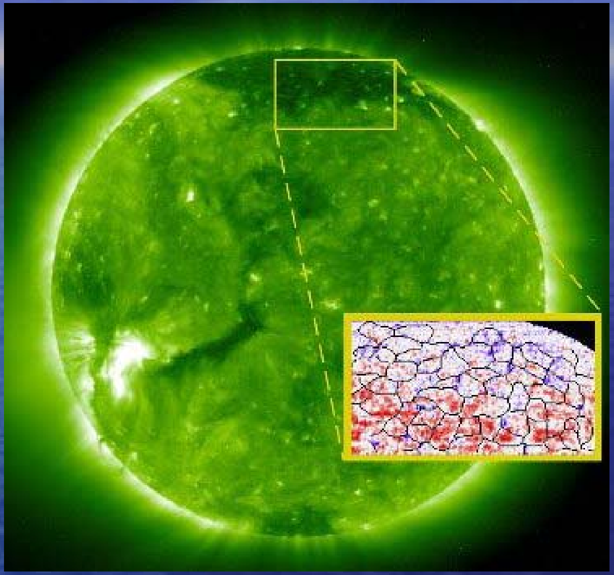

Blue regions are inside a coronal hole or open magnetic field region, where the high-speed solar wind is accelerated. Superposed are the edges of "honeycomb"- shaped patterns of magnetic fields at the surface of the Sun, where the strongest flows occur.

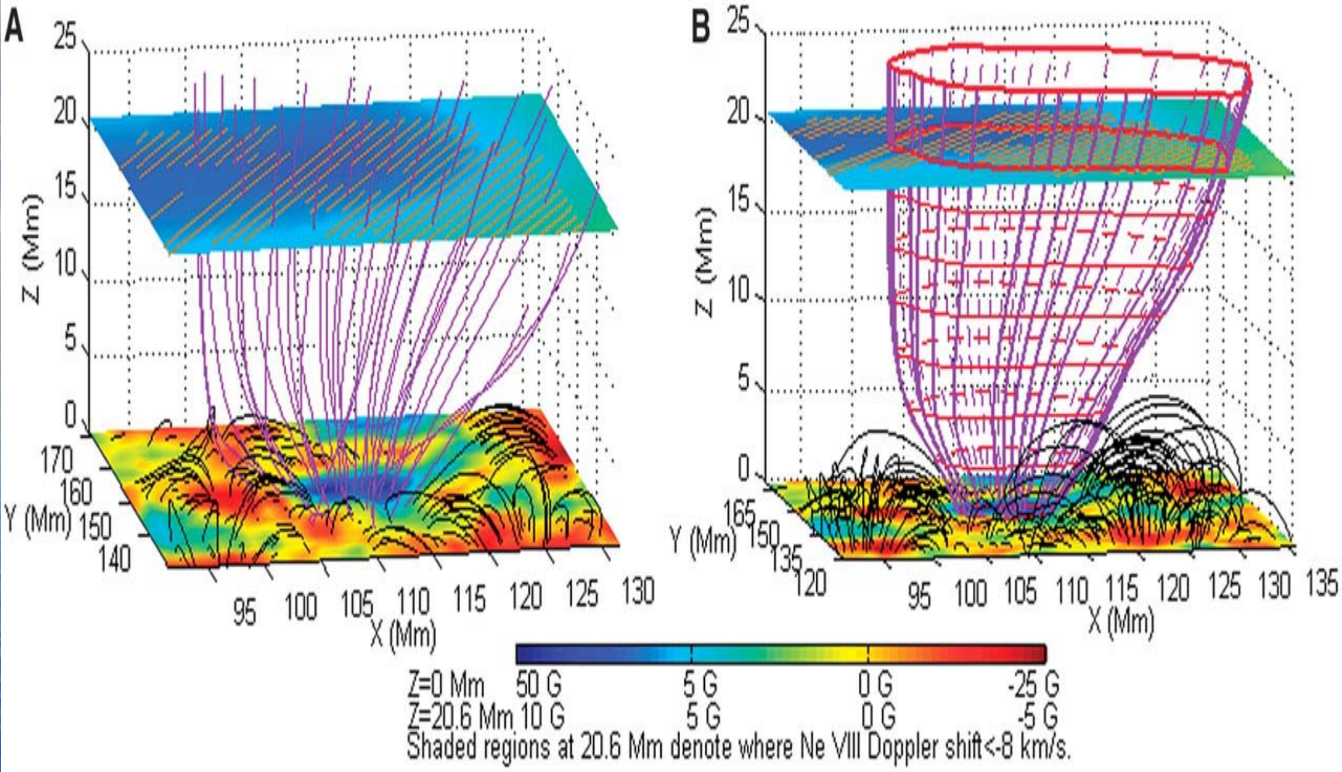

The solar wind starts flowing out of the corona at heights above photosphere between 5 Mm and 20 Mm in magnetic funnels. (Tu *et al.,* 2005).

Signature of MHD Waves in Polar Coronal Holes

- **Moran (2003) --- Line widths from ions formed at coronal hole temperatures increase with height up to 1.1 R $_{\odot}$; & constant at > 1.1 R $_{\odot}$.**

  Line broadening --- Alfvén wave propagation.

  Waves are damped > 1.1 R $_{\odot}$.

- **O'Shea et al. (2005) --- Evidence for a decrease in line widths at height above the limb ~ 1150´´ (~1.2 R $_{\odot}$) in polar regions where Mg X 624/609 indicates a change from a collisionally to a radiatively dominant excitation mechanism.**

This decrement in the line widths above ~1150´´ (~1.2 R $_{\odot}$) is likely due to a reduction in the non-thermal component of the line widths caused by a damping of upwardly propagating Alfvén waves.

- **EIT Fe IX and Fe X 171 Å observation (DeForest and Gurman 1998) --- propagating disturbances (periods 10-15 min) in plume regions --- Signatures of quasi-periodic compressional waves --- slow magnetosonic waves (Ofman *et al.*, 1999; Ofman and Deforest, 2000).**

- **UVCS white light channel (Ofman *et al.*, 2000) --- Evidence of periodic density fluctuations with periods ~ 30 min in polar coronal holes --- consistent with propagating slow magnetosonic waves at 1.9 $R_\odot$.**

- **Signatures of long period (20-60 min and above), and very long period (170 min) periodic fluctuations obtained (Banerjee *et al.*, 2001; Popescu *et al.*, 2005).**

- **O'Shea *et al.* (2006) --- Evidence for fast magnetoacoustic waves at coronal temperatures, while at transition region temperatures slow magnetoacoustic waves are more common.**

  Strong evidence for outwardly propagating slow magnetoacostic waves in off-limb polar regions.

MHD equations for viscous and resistive plasma :

$$\rho\frac{\partial \mathbf{v}}{\partial t} + \rho\left(\mathbf{v}\cdot\nabla\right)\mathbf{v} = \frac{1}{\mu}\left(\nabla\times\mathbf{B}\right)\times\mathbf{B} + \rho\,\nu\nabla^2\,\mathbf{v}$$

(momentum equation)

$$\frac{\partial \mathbf{B}}{\partial t} = \nabla\times\left(\mathbf{v}\times\mathbf{B}\right) + \eta\nabla^2\,\mathbf{B}$$

(induction equation)

and

$$\nabla\cdot\mathbf{B} = 0$$

Linearized equations :

$$\rho_o \frac{\partial \mathbf{v}_1}{\partial t} = \frac{1}{\mu}\left(\mathbf{B}_o \cdot \nabla\right)\mathbf{B}_1 + \rho_o \ \nu \nabla^2 \mathbf{v}_1$$

and

$$\frac{\partial \mathbf{B}_1}{\partial t} = \left(\mathbf{B}_o \cdot \nabla\right) \mathbf{v}_1 + \eta \nabla^2 \mathbf{B}_1$$

Assuming plane wave solutions

$$\mathbf{v}_1 = \mathbf{v}_{max} \exp\left[i\left(\mathbf{k}\cdot\mathbf{r}-\omega t\right)\right]$$

and

$$\mathbf{B}_1 = \mathbf{B}_{max} \exp\left[i\left(\mathbf{k}\cdot\mathbf{r}-\omega t\right)\right]$$

we get the dispersion relation :

$$\nu\eta k^4 + \left[v_A^2 - i\omega\left(\nu+\eta\right)\right]k^2 - \omega^2 = 0$$

where $v_A = \frac{\mathbf{B}}{\sqrt{\mu\rho}}$ **is Alfvén velocity**

If we consider the effect of viscosity only, we get

$$k_r^{\,4} - P k_r^{\,2} - Q^2 = 0$$ **and** $$k_r \times k_i = Q$$

where $$P = \frac{\omega^2 v_A^{\,2}}{v_A^{\,4} + \omega^2 \nu^2}$$ **and** $$Q = \frac{\omega^3 \nu}{2(v_A^{\,4} + \omega^2 \nu^2)}$$

If we consider the effect of magnetic diffusivity only, we get

$$k_r^{\,4} - P' k_r^{\,2} - Q'^2 = 0$$ **and** $$k_r \times k_i = Q'$$

where $$P' = \frac{\omega^2 v_A^{\,2}}{v_A^{\,4} + \omega^2 \eta^2}$$ **and** $$Q' = \frac{\omega^3 \eta}{2(v_A^{\,4} + \omega^2 \eta^2)}$$

$$\rho \nu = 1.0045 \times 10^{-16}\, T_R^{\,2.5} \ \text{g cm}^{-1}\, \text{s}^{-1}$$ **(Spitzer, 1962)**

$$\eta = 1.144 \times 10^{13}\, T_R^{\,-1.5} \ \text{cm}^2\, \text{s}^{-1}$$ **(Priest, 1982).**

Density profile in a polar coronal hole as a function of radial height (Doyle *et al.* , 1999) :

$$N_e(R) = \frac{1\times10^8}{R^8} + \frac{2.5\times10^3}{R^4} + \frac{2.9\times10^5}{R^2} \quad (\mathrm{cm}^{-3})$$

where mass density

$$\rho_o(R) = 0.6\, m_p\, N_e(R)$$

The empirical relation for temperature profile is given by Pekünlü *et al.* (2002) in coronal holes, using David *et al.* (1998) temperature measurements:

$$T_R = -2\times10^7\ R^2 + 5\times10^7\, R - 3\times10^7\ (K)$$

Energy flux density of Alfvén wave

$$W = \rho v_{\rm NT}^2(R)\frac{\partial \omega}{\partial k}$$, where $\frac{\partial \omega}{\partial k}$ is group velocity

and $v_{\rm NT}(R)$ is velocity equivalent of the non-thermal component of relevant spectral line at FWHM.

We use the empirical relation as a function of radial height, given by Pekünlü *et al.* (2002) using Banerjee *et al.* (1998) measurements for Si VIII ion :

$$v_{\rm NT}(R) = -15223R^4 + 86382R^3 - 181191R^2 + 16882R - 57865 \ (\mathrm{km\,s^{-1}})$$

We consider the coronal hole region in two parts. The lower part below 25 Mm is coronal funnel, having open magnetic field lines with complex bipolar magnetic structures (Tu *et al.*, 2005). The magnetic structure of the upper part of coronal funnel (above 25 Mm) is quite homogeneous (Banaszkiewicz *et al.* 1998; Hackenberg *et al.* 2000). We then derive an empirical relation for the magnetic field in the inner coronal hole as :

$$B = \frac{a}{1 + \exp\left[(R-b)/c\right]} + d$$

for 1.00 $R_\odot$ < R < 1.05 $R_\odot$, (gauss)

$$B = 95.20344 - 129.39079\,R + 45.49857\,R^2$$

for 1.05 $R_\odot$ < R < 1.35 $R_\odot$

- We take 1.05 $R_\odot$ as a reference height and make all the physical quantities dimensionless, by dividing the respective values

i.e., $T, \eta, \nu, v_{\mathrm{A}}, \rho, B$ and v_{NT}

at R = 1.05 $R_\odot$, for example, $T_R \rightarrow \dfrac{T_R}{T_{R=1.05 R_o}}$ etc.

- We also consider the shortest period

$\tau_{\mathrm{A}\,ref} = 0.01$ s

as a reference time to make the time periods dimensionless, i.e., $\tau_{\mathrm{A2}} \rightarrow \tau_{\mathrm{A2}} / \tau_{\mathrm{A}\,ref}$, $\tau_{\mathrm{A3}} \rightarrow \tau_{\mathrm{A3}} / \tau_{\mathrm{A}\,ref}$ etc

- We use these dimensionless physical quantities in the dispersion relation and calculate the wave number, which is actually

$$k_{\text{mod}} \approx \frac{k_{\tau_{\text{A}},R}}{k_{\tau_{\text{A ref}},R_{ref}}}$$

- Following equations convert the physical parameters in cgs units

$$D_{\tau_{\text{A}},R} \approx \frac{1}{2\pi} \times D \times D_{\tau_{\text{A}\ ref},R_{ref}} \qquad \text{(cm)}$$

$$W_{\tau_{\text{A}},R} \approx \frac{1}{2\pi} \times W \times W_{\tau_{\text{A}\ ref},R_{ref}} \qquad (\text{ergs cm}^{-2}\ \text{s}^{-1})$$

and

$$V_{g\,\tau_{\text{A}},R} \approx \frac{1}{2\pi} \times V_g \times V_{g\,\tau_{\text{A}\ ref},R_{ref}} \qquad (\text{cm s}^{-1})$$

Spatial Variation of Damping Length Scale

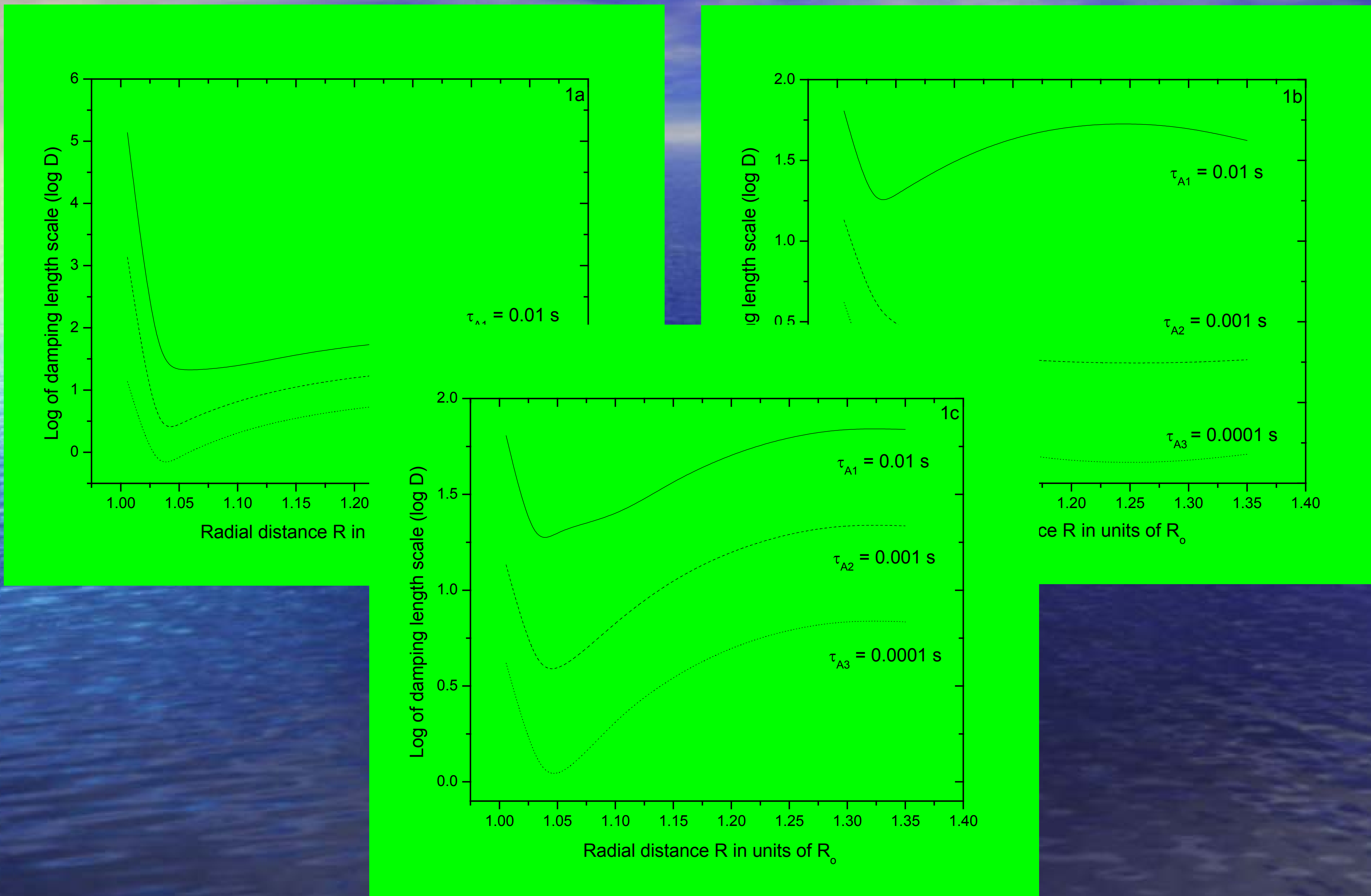

Spatial Variation of Energy Flux Density and Non-thermal Velocity

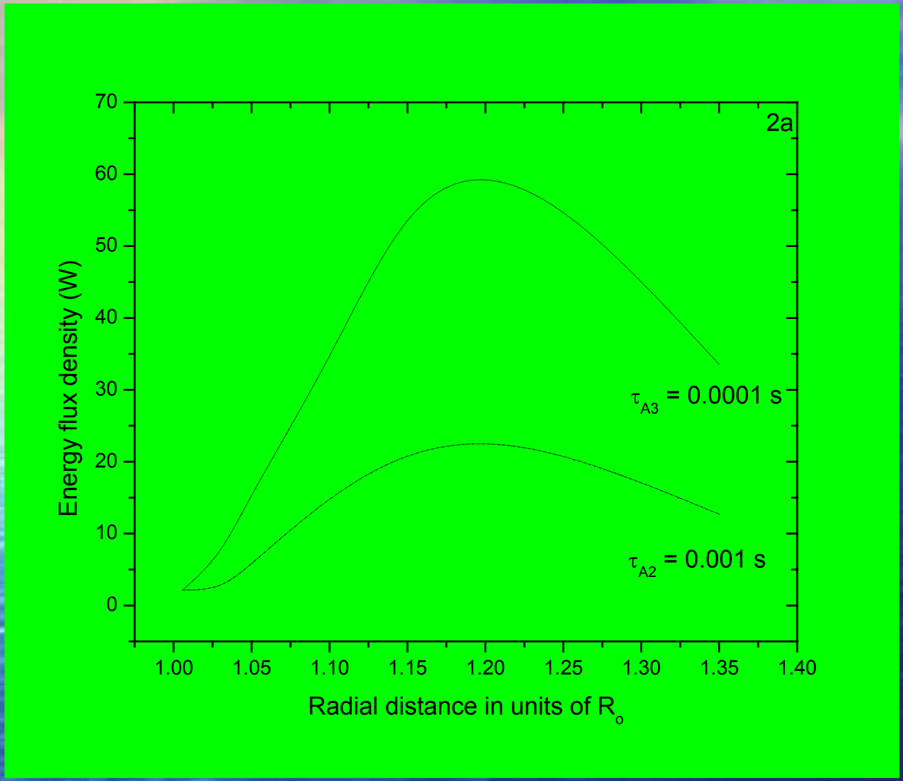

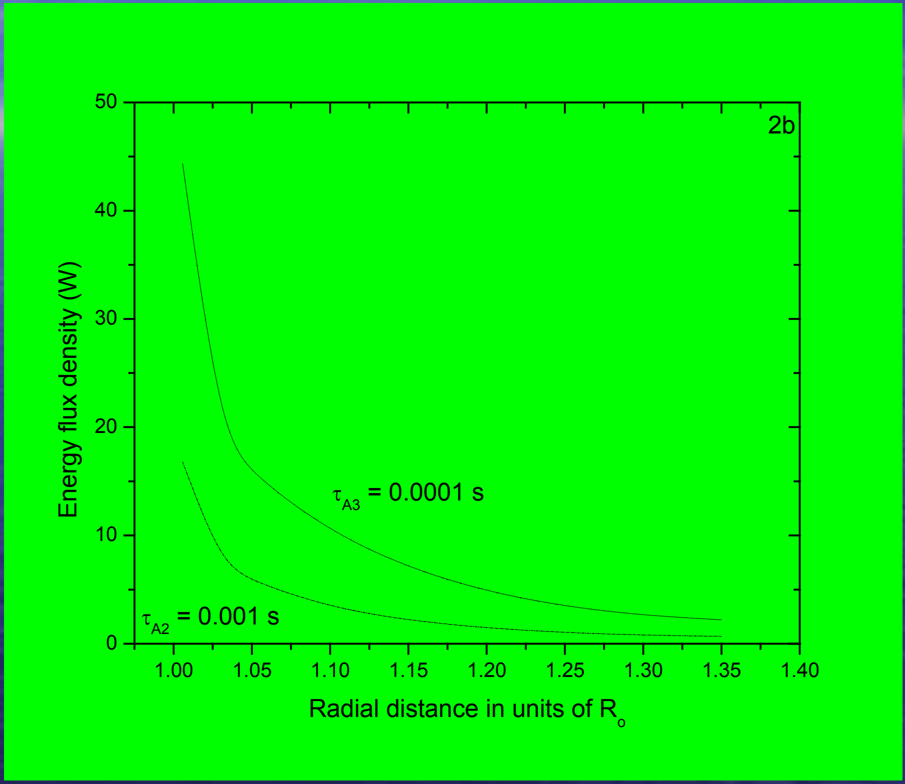

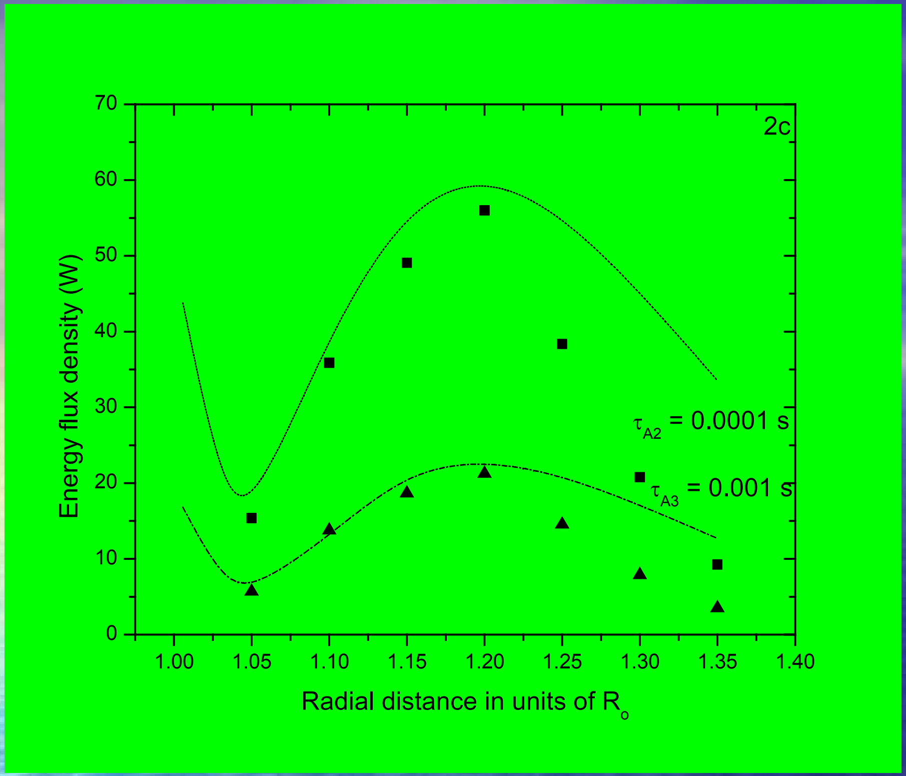

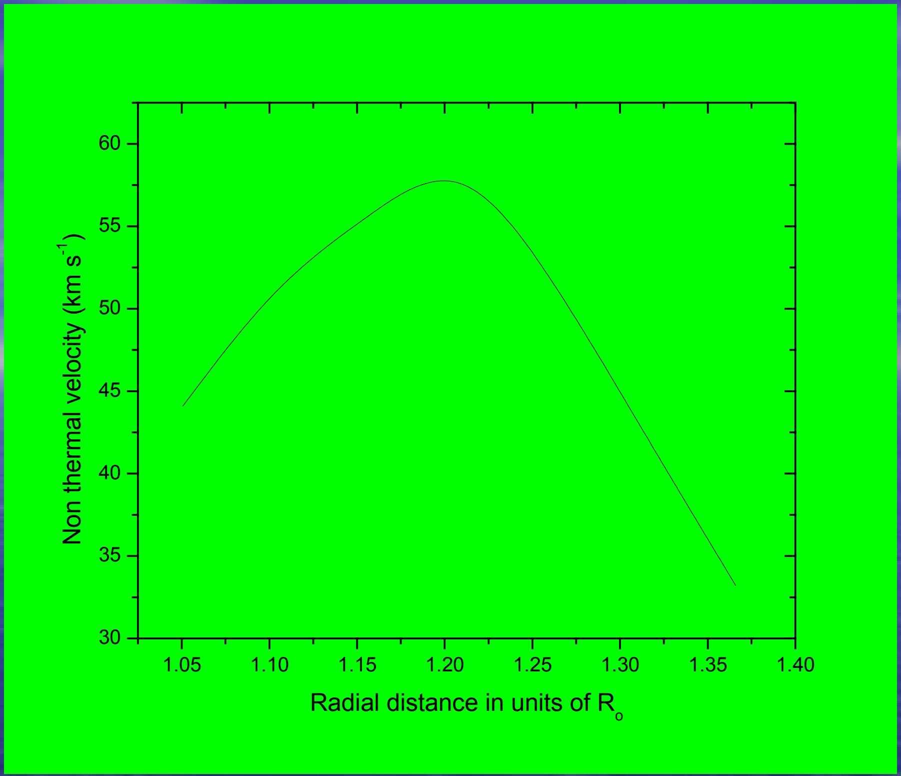

Non-thermal velocity is deduced by using

$$\frac{2kT}{M} + \xi^2 = \frac{1}{4\ln 2} c^2 \left(\frac{\Delta\lambda}{\lambda}\right)^2$$

Spatial Variation of Group Velocity

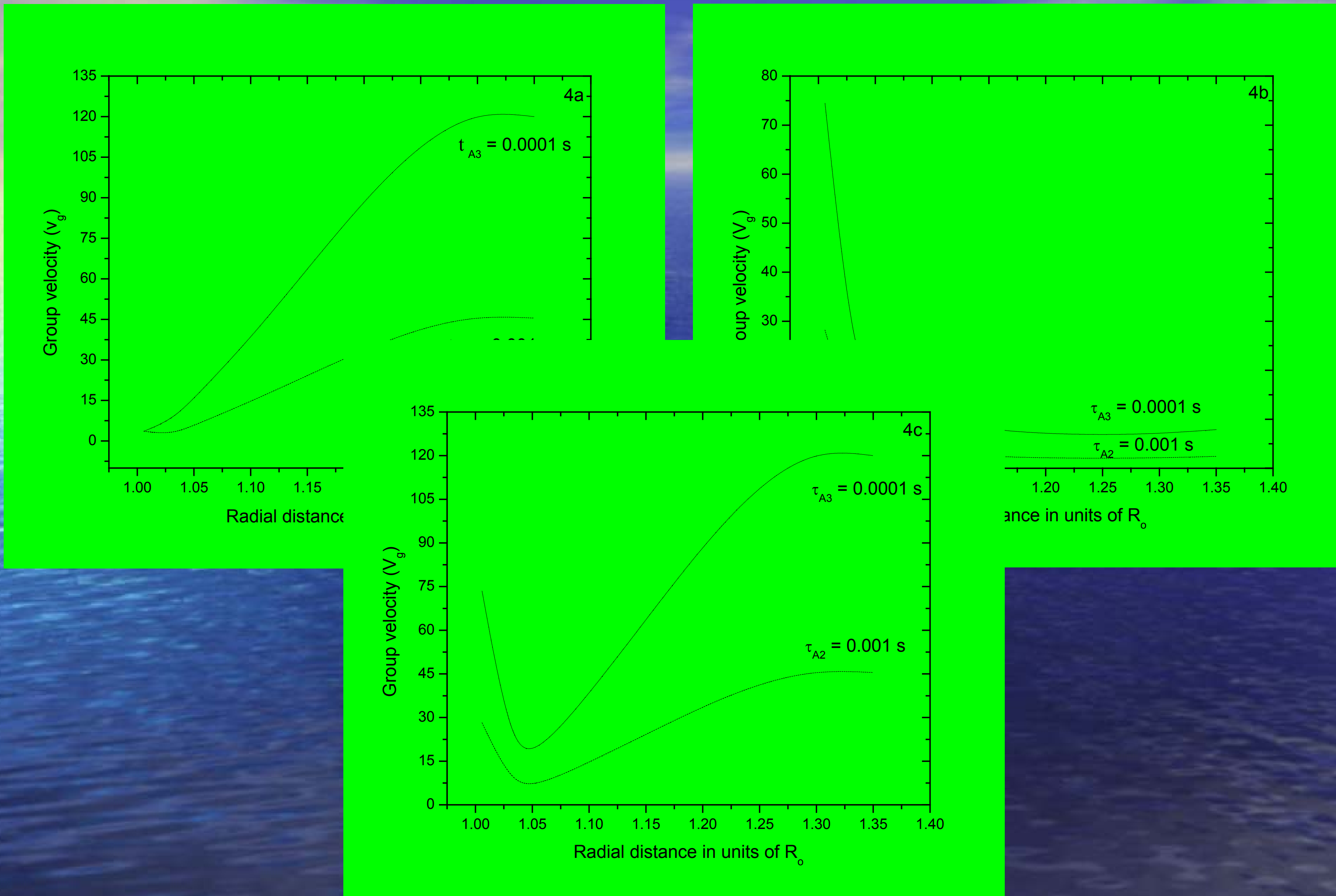

Alfvén Waves Propagating at Different Angles

More general dispersion relation for the obliquely propagating Alfvén waves :

$$P\,k^4 + Q\,k^2 - \omega^2 = 0$$

where $P = \nu\,\eta\,\cos^4\theta,$ $Q = \left[v_A^{\;2} - i\,\omega\left(\nu+\eta\right)\right]\cos^2\theta$

and $v_A = \dfrac{B}{\sqrt{\mu\rho}}$ **Alfvén velocity.**

Spatial variation of damping length scale, energy flux density & group velocity of Alfvén waves, propagating at different angles

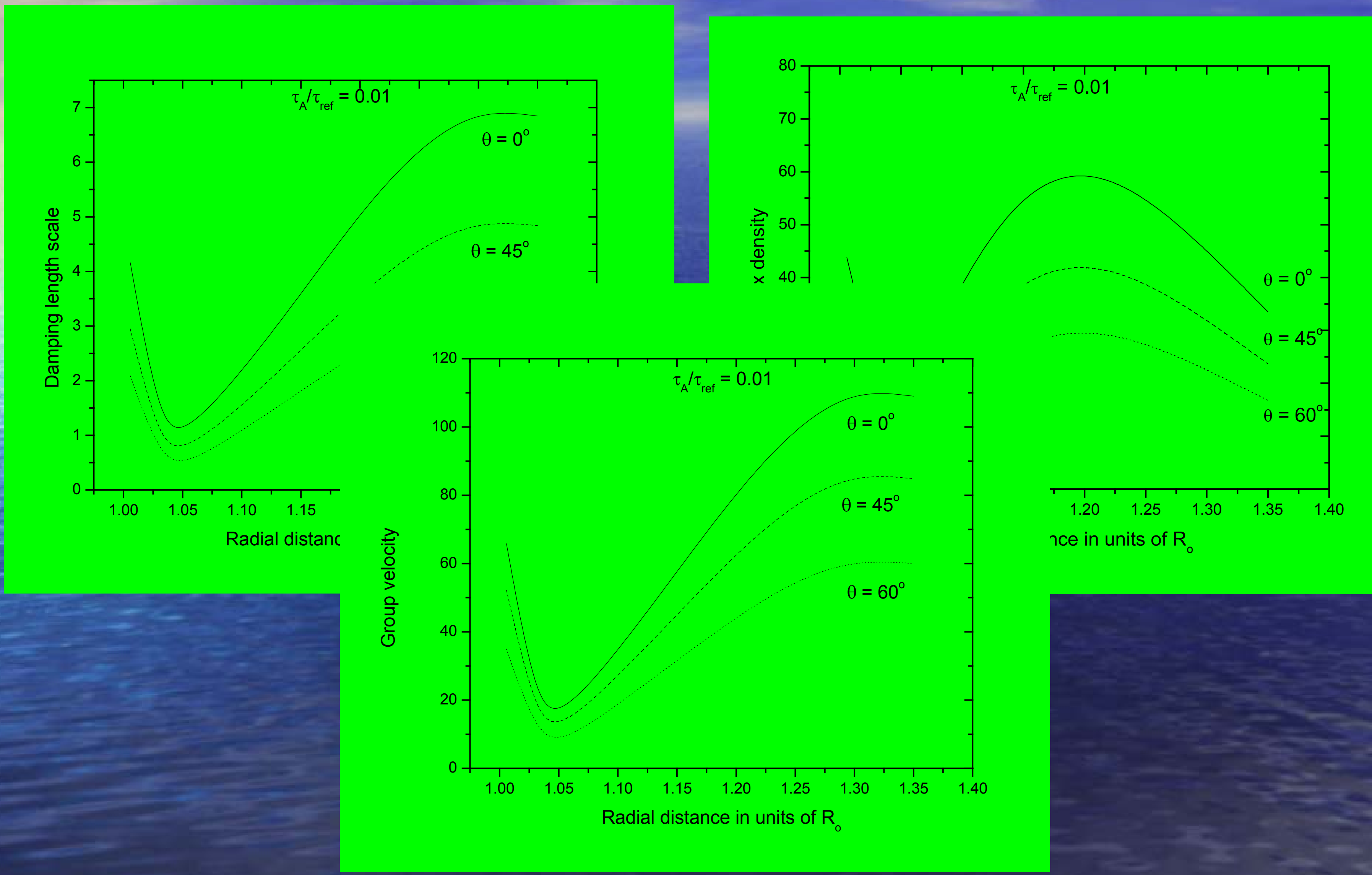

Results

The outward propagating Alfvén wave propagation and dissipation in magnetic funnels through viscous and resistive plasma --- Alfvén waves are one of the primary energy sources in the innermost part of coronal holes where the solar wind outflow starts.

Spectroscopic signature of Alfvén wave dissipation in the off-limb coronal hole plasma --- Alfvén waves with period 0.0 01 s fit the data best.

Long Period Slow MHD Waves in Solar Wind Source Region

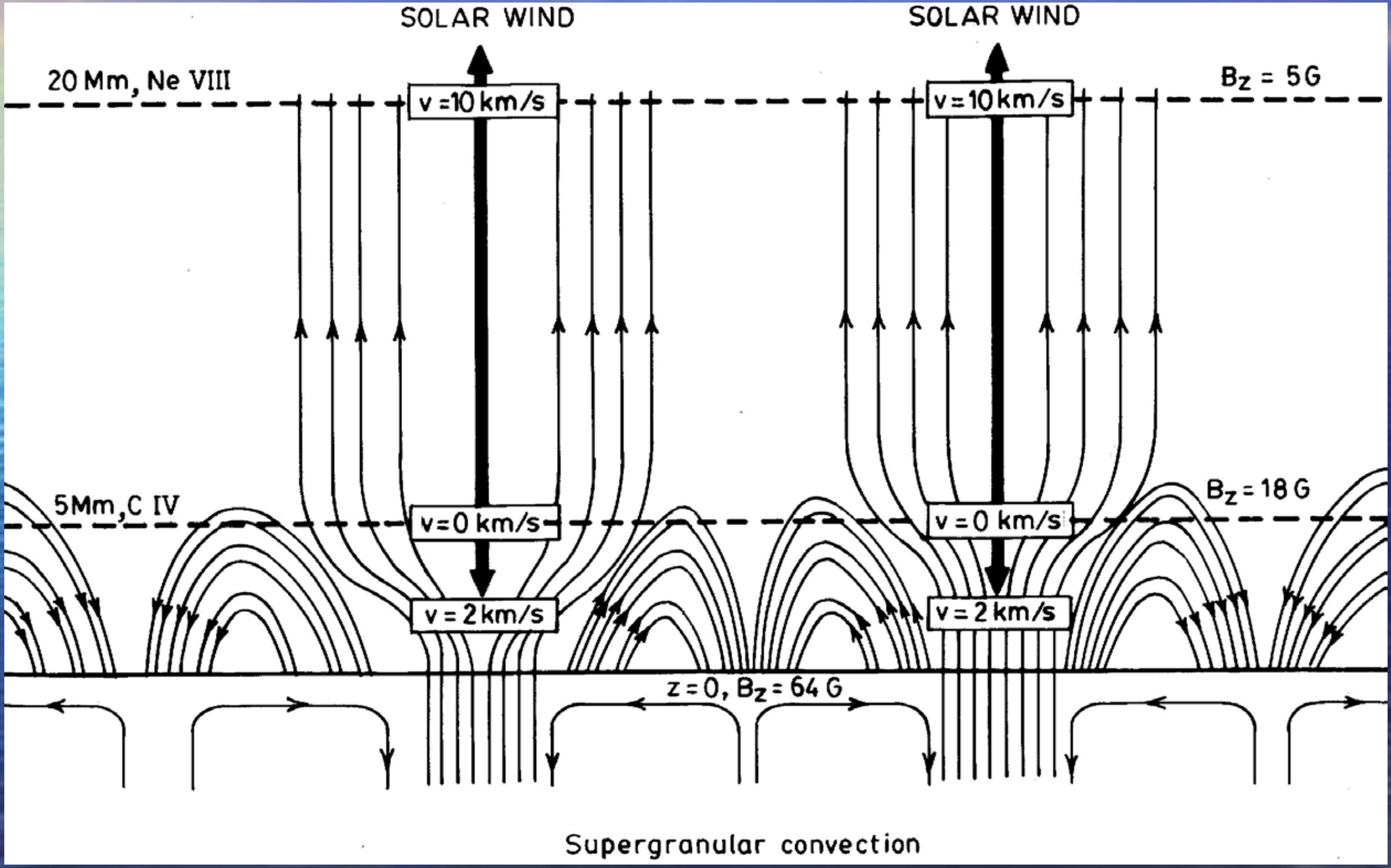

Doppler line widths of radially outward propagating Alfvén waves, and slow longitudinal MHD waves are : (e.g., Erdélyi *et al.* 1998)

$$\Delta\lambda_{D\ Alf} = \frac{1}{c}\left(\frac{2kT}{M_i} + \frac{4\pi^{0.5}\phi_{Alf}}{\rho^{0.5}B}\right)^{0.5}\lambda$$

$$\Delta\lambda_{D\ Lon} = \frac{1}{c}\left(\frac{2kT}{M_i} + \frac{2\phi_{Lon}}{N_e(6m_p kT)^{0.5}}\right)^{0.5}\lambda$$

We take $c = 3\times10^{10}$ cm s^{-1} , $k = 1.38\times10^{-16}$ ergs K^{-1} , $M_i = 4.008\times10^{-24}$ g for Mg X ion, $\lambda = 609.78$ Å, proton mass $m_p = 1.67\times10^{-24}$ g.

ϕ_{Alf} is energy flux density for Alfvén waves.

ϕ_{Lon} is energy flux density for slow MHD waves.

Using density, temperature profiles

$$N_e(R) = \frac{1\times10^8}{R^8} + \frac{2.5\times10^3}{R^4} + \frac{2.9\times10^5}{R^2} \quad (\mathrm{cm}^{-3})$$

(Doyle *et al.*, 1999)

Mass density,

$$\rho_o(R) = 0.6\, m_p\, N_e(R)$$

(where m_p is the proton mass)

$$T_R = -2\times10^7\, R^2 + 5\times10^7\, R - 3\times10^7 \ K$$

(Pekünlü *et al.* 2002)

Dispersion Relation

$$Ak^6 + Bk^4 + Ck^2 + D = 0,$$

with coefficients ,

$$A = \frac{4}{3} i \gamma^2 \varepsilon d + \frac{16}{9} \gamma^3 \varepsilon^2 \omega d$$

$$B = \gamma^2 \omega d + \frac{4}{3} \gamma^2 \omega \varepsilon - \frac{8}{3} i \gamma^3 \omega^2 \varepsilon d - \frac{16}{9} i \gamma^2 \omega^2 \varepsilon^2$$

$$C = -\gamma^3 \omega^3 d - \frac{8}{3} \gamma^2 \omega^3 \varepsilon - i \omega^2 \gamma^2$$

$$D = i \gamma^2 \omega^4 .$$

where the two parameters are :

$$\varepsilon = \frac{\eta_o \tau}{\rho_o L^2} = \frac{\eta_o}{\gamma \tau p_o}$$

(where $L = c_s \tau$ **and** $c^2{}_s = \gamma p_0 / \rho_0$ **)**

$$d = \frac{(\gamma - 1)\kappa_{\|} T_o \rho_o}{\gamma^2 p_o{}^2 \tau}$$

and we use

$$\eta_o = 10^{-16} T_o{}^{2.5}$$

(g cm^{-1} s^{-1})

$$\kappa_{\|} = 10^{-6} T_o{}^{2.5}$$

(ergs cm^{-1} s^{-1} K^{-1}) (Braginskii 1965)

Linearized equations (DeMoortel and Hood, 2003)

$$\frac{\partial v_1}{\partial t} = -\frac{1}{\gamma}\frac{\partial p_1}{\partial z} + \frac{4}{3}\varepsilon \frac{\partial^2 v_1}{\partial z^2}$$

$$\frac{\partial \rho_1}{\partial t} = -\frac{\partial v_1}{\partial z}$$

$$\frac{\partial T_1}{\partial t} = -(\gamma - 1)\frac{\partial v_1}{\partial z} + \gamma d \frac{\partial^2 T_1}{\partial z^2}$$

$$p_1 = \rho_1 + T_1$$

to obtain the dispersion relation. We solve these equations simultaneously, assuming all variables to have phase factor

$$exp(ikz - i\omega t).$$

One-dimensional MHD equations (DeMoortel and Hood, 2003)

$$\rho \frac{\partial \mathrm{v}}{\partial t} + \rho \mathrm{v} \frac{\partial \mathrm{v}}{\partial z} = - \frac{\partial \mathrm{p}}{\partial z} + \frac{4}{3} \eta_o \frac{\partial^2 \mathrm{v}}{\partial z^2}$$

$$\frac{\partial \rho}{\partial t} = - \frac{\partial}{\partial z} (\rho \mathrm{v})$$

$$\frac{\partial \mathrm{p}}{\partial t} + \mathrm{v} \frac{\partial \mathrm{p}}{\partial z} = - \gamma \mathrm{p} \frac{\partial \mathrm{v}}{\partial z} + (\gamma - 1) \frac{\partial}{\partial z} \left(\kappa_{\parallel} \frac{\partial T}{\partial z} \right)$$

$$p = \frac{\rho}{\tilde{\mu}} R T$$

$$W = \rho v_{NT}^2 (R) \ V$$ **(energy flux density)**

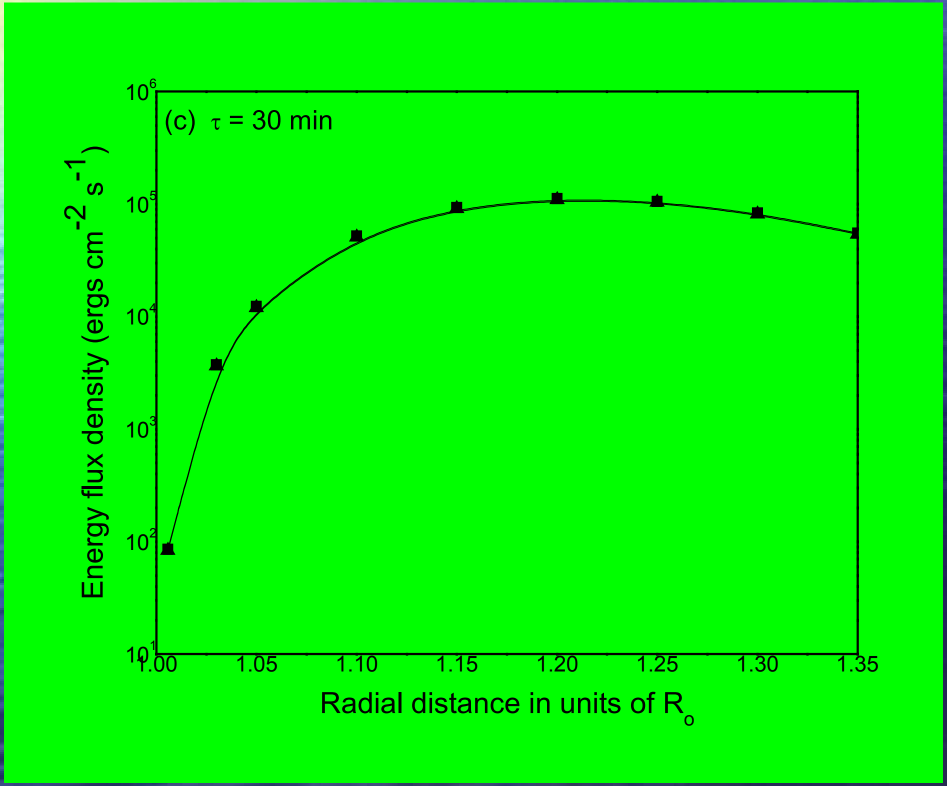

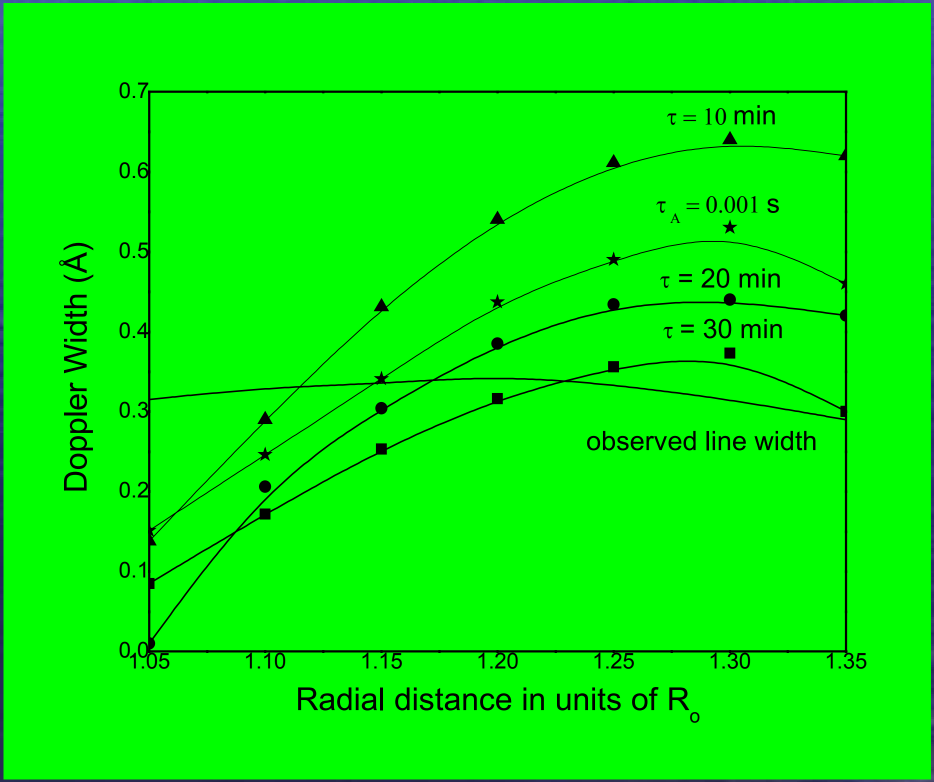

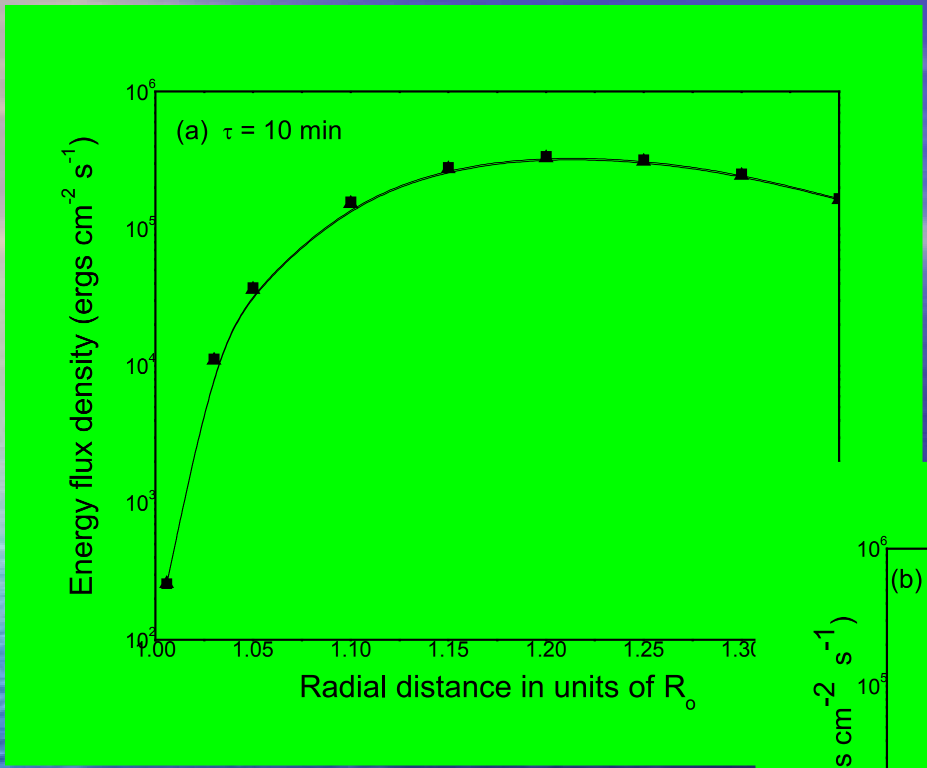
(a) τ = 10 min
Energy flux density (ergs cm^-2 s^-1)
Radial distance in units of R_o

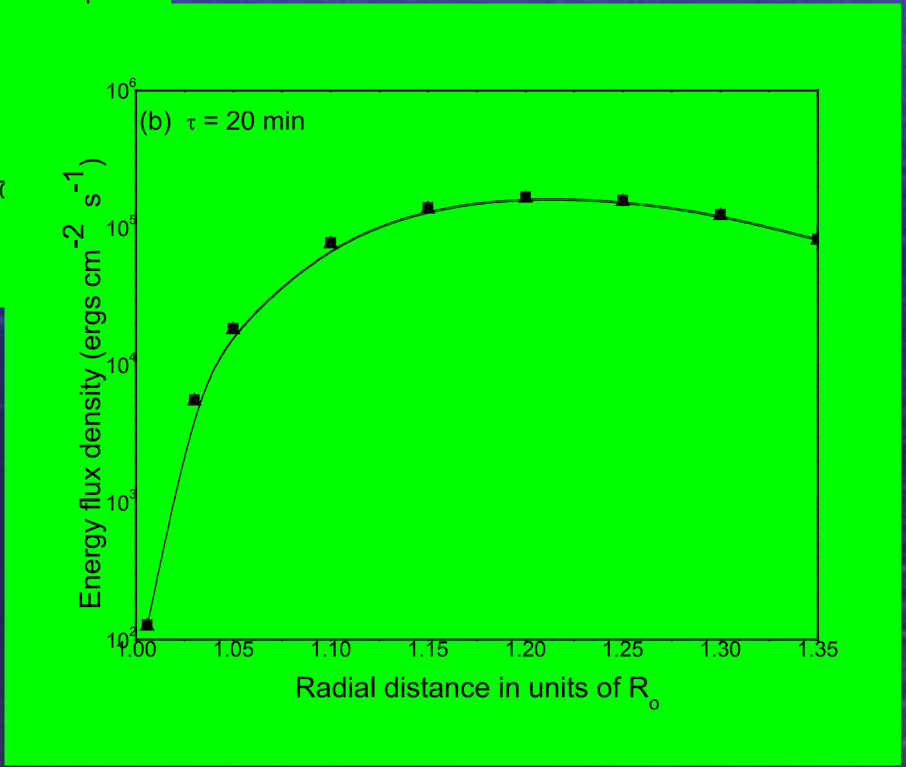
(b) τ = 20 min
Energy flux density (ergs cm^-2 s^-1)
Radial distance in units of R_o

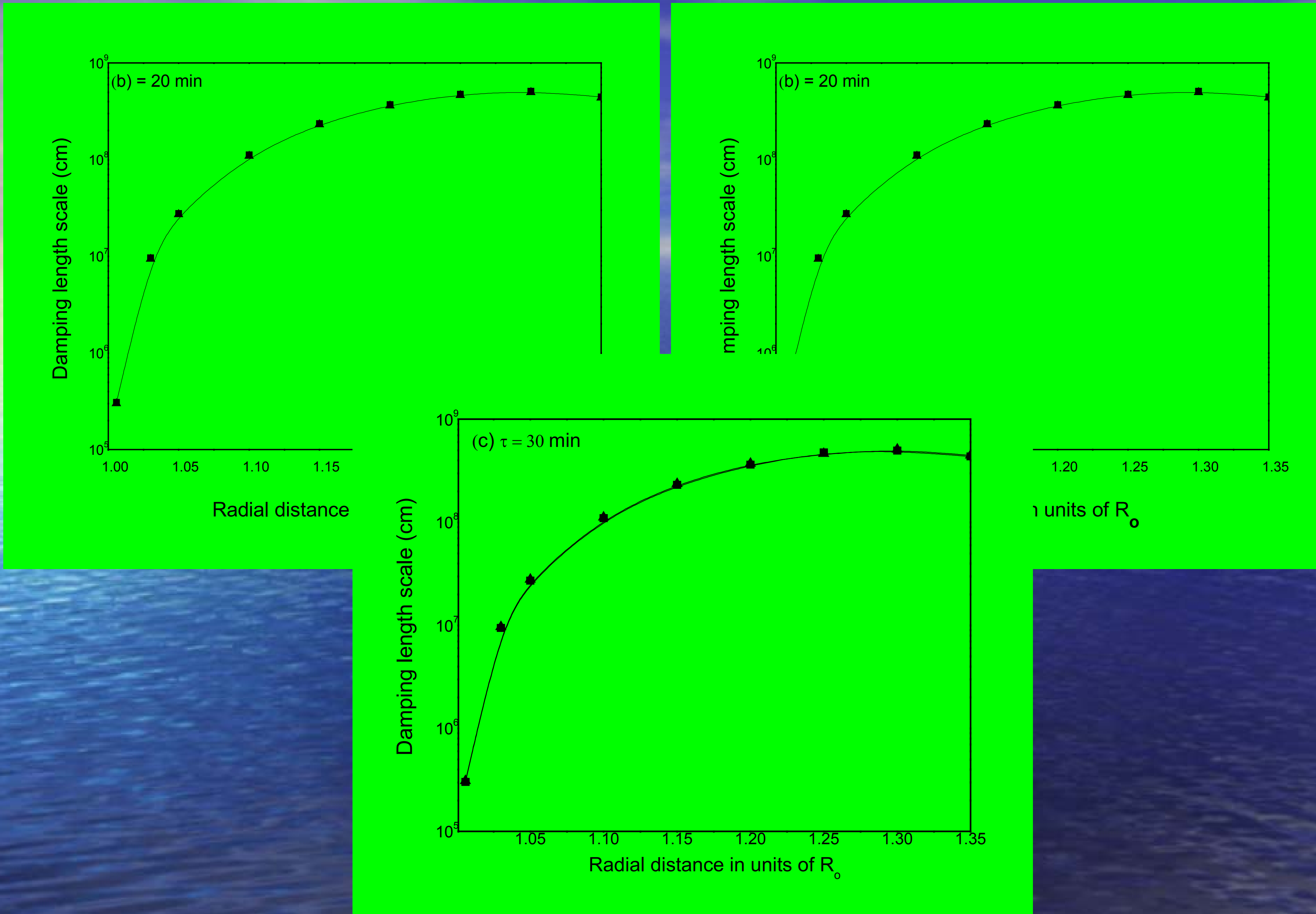
(b) = 20 min
Damping length scale (cm)
Radial distance
(b) = 20 min
mping length scale (cm)
units of R
(c) τ = 30 min
Damping length scale (cm)
Radial distance in units of R
1.00
1.05
1.10
1.15
1.20
1.25
1.30
1.35

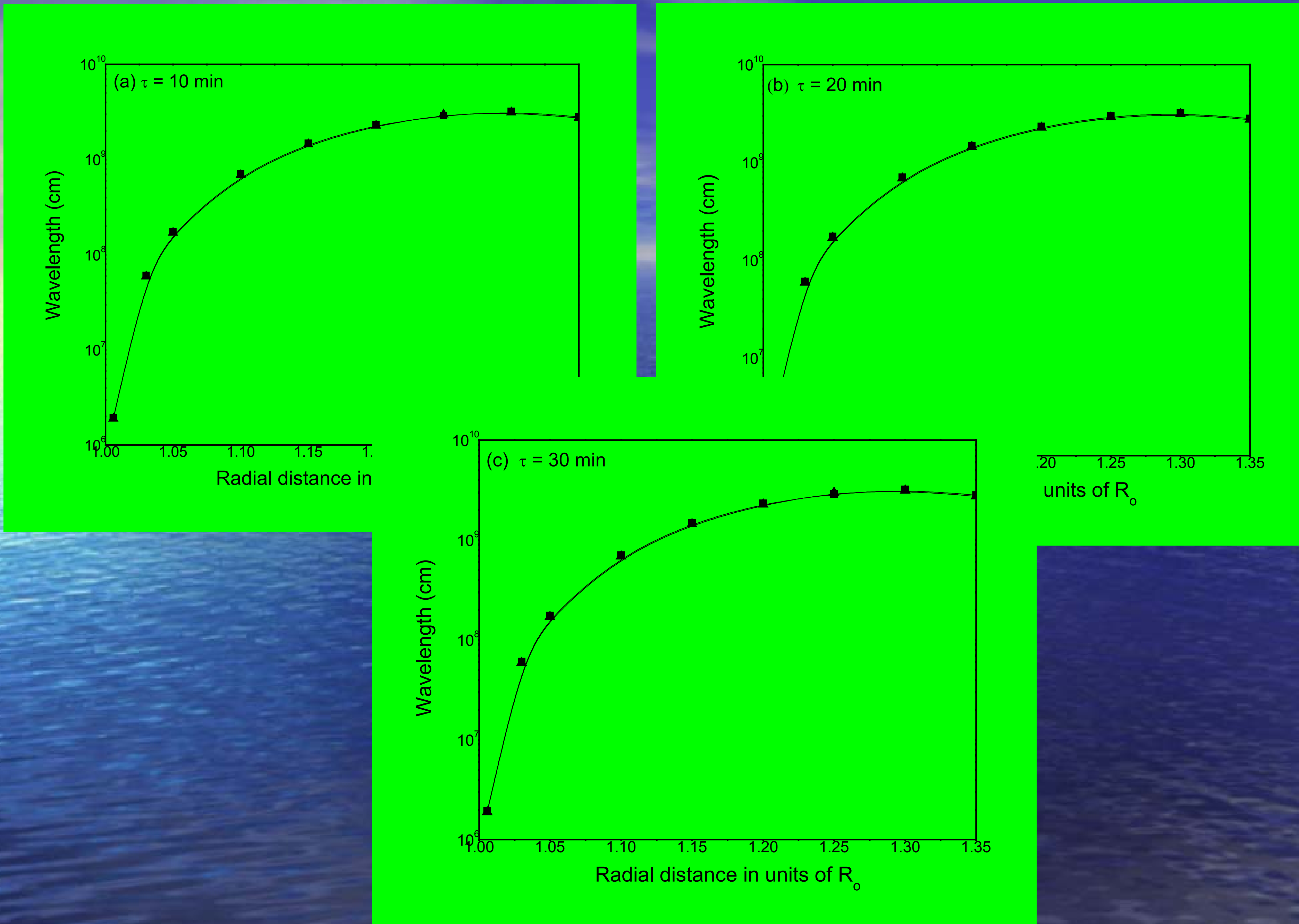
(a) τ = 10 min
Wavelength (cm)
Radial distance in
(b) τ = 20 min
Wavelength (cm)
units of R_o
(c) τ = 30 min
Wavelength (cm)
Radial distance in units of R_o
10^{6}
10^{7}
10^{8}
10^{9}
10^{10}
1.00
1.05
1.10
1.15
1.20
1.25
1.30
1.35

Results

- Slow longitudinal MHD waves also contribute to the observed line profile narrowing. The wave with period 30 min fits the data best.

- In solar wind source region (1.0058 $R_{\odot}$ - 1.03 $R_{\odot}$) --- only Alfvén waves are likely candidates.

- Slow longitudinal waves are important in upper part of solar wind source region (1.03 $R_{\odot}$ - 1.35 $R_{\odot}$), providing a fraction of the required energy --- dissipation of both types of waves in coronal holes.


Thank You